Geometry and characterization of wrinkles in paper

Craig R. Friedrich
Assistant professor, Dept. of Mechanical Engineering, Louisiana Tech University, Ruston, La. 71272

ABSTRACT *The normal elastic equations are based on the assumption of small displacement and thus are not useful in describing the large deformation that occurs in a web wrinkle. The equations of the elastica can be used to describe the geometry of a wrinkle, but these equations are difficult to use on a repetitive basis. In this study, the cross-sectional geometry of a number of wrinkles in several types of paper was measured and normalized. This process yielded a simple polynomial relationship that can be easily used to describe the general shape of a web wrinkle. Comparison of the wrinkle shapes predicted by the polynomial and by the elastica with the measured wrinkles showed good agreement. The results provide a very easy method for characterizing and predicting a wrinkle cross-section in the modeling of paper wrinkles.*

KEYWORDS
Creasing
Geometry
Mathematical models
Paper webs
Tension control
Web tension
Wrinkles

In the study of the behavior of wrinkles in paper and other web materials, the assumed shape of the wrinkle is important in modeling the wrinkle's interaction with rollers and other geometric variables of the processing line. Past work has shown that the behavior of a wrinkle is heavily dependent on the shape of the wrinkle cross-section (*1*). One of the parameters addressed in this earlier work is the wrinkle aspect ratio, which is defined as the total wrinkle height divided by the total wrinkle width. It was learned that as the aspect ratio increased, the behavior of the wrinkle became less stable, and the wrinkle was more prone to creasing or collapsing when passing over a roller. The assumed mathematical function for the cross-sectional shape was a simple sinusoid. This simplified assumption was useful in determining the relative contribution of several parameters to wrinkle stability. However, as research into wrinkle stability has progressed, the need for a more accurate description of the wrinkle shape has become apparent.

Wrinkling can be created by a number of processing factors, including misaligned rollers, eccentric rollers, uneven tension profile, active steering and guiding, and other elements that induce shear strain into the web. In all cases, the initiation of wrinkling can be consolidated into one general cause. Wrinkling is initiated when the compressive stress in the entire web (or a portion of the web) exceeds the stress at which the material will structurally buckle.

In most engineering applications, buckling is considered to be a failure mode because deflection is no longer linearly proportional to the applied load. At the initiation of structural buckling, the out-of-plane deflection can be quite small, but the condition is still considered to be in a state of unstable equilibrium. In paper, the buckling load is extremely small, and the out-of-plane deflection at theoretical buckling is also very small. A wrinkle with such a small amplitude will probably not even be noticed unless the localized weakness allows transfer of the compressive stress to adjacent regions of the web. If this happens, the wrinkle is likely to grow in both width and amplitude.

As shown in the previous work (*1*), if the ratio of height to width approaches some threshold value, then the wrinkle may exhibit an adverse behavior when encountering out-of-plane guiding, such as passing over a roller. However, it is not sufficient to know just the total height and total width of a wrinkle in attempting to predict wrinkle behavior. It is also necessary to describe the height of the wrinkle at any point in the wrinkle cross-section.

Classical plate buckling

In the classical development of the buckling behavior of thin plates, the unbuckled plate is subjected to external, in-plane loads. As the external loads approach the critical value, the work performed by the loads is manifested by planar deformation of the

1. Model for large-deflection buckling, or wrinkling, as described by the *elastica*

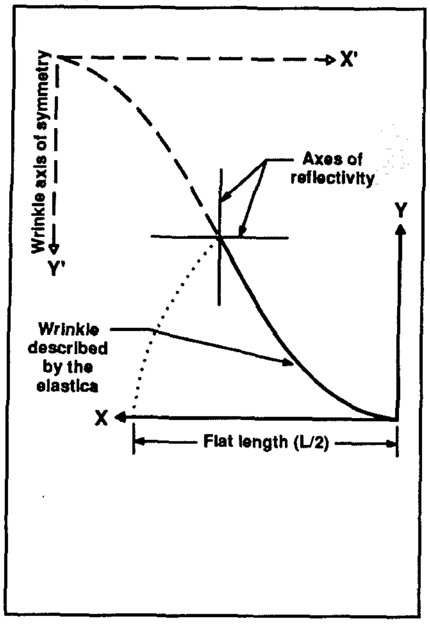

2. Wrinkle-formation apparatus

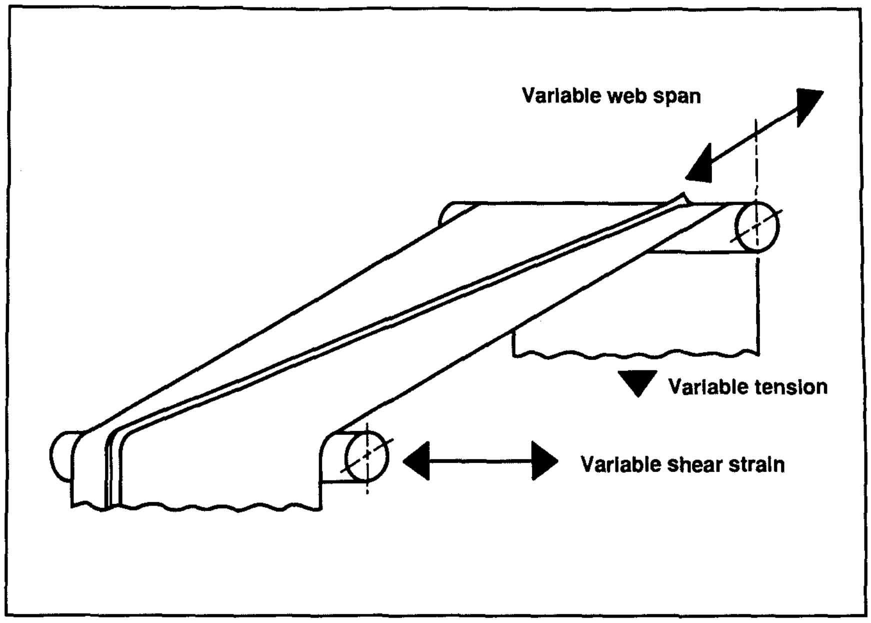

plate. When the loads reach a critical value, the plate suddenly deforms out of the plane of the plate. This deformation is consistent with the principle that the plate deforms such that: (a) the potential energy of the loads and of the deformed plate is a minimum, and (b) the work done by the external loads is equal to the strain energy stored in the plate.

In this development, it is necessary to assume a buckled shape for the plate. A solution composed of an infinite series of sinusoidal functions, which satisfy the boundary conditions for the plate, is nearly always assumed. This development can be found in many references on thin-plate buckling (*2-5*).

The assumed sinusoidal function is appropriate for buckling deformations that are still in the structural regime. This implies that buckling is a failure mode to be avoided and that the post-buckling shape is of little interest. In addition, the simplifying assumption of small deflection in the buckled state introduces a degree of uncertainty regarding the shape of the out-of-plane deformation. This simply means that the buckled shape cannot be uniquely described (*5*).

In paper wrinkles, the post-buckling shape is important because buckling, in itself, is not considered to be a structural or material failure. The classical elastic equations of plate behavior do not adequately describe the wrinkle behavior because the plate equations are based on the simplifying assumption of small deformation. For plates, small deformation is on the order of the plate thickness. For paper wrinkles, the out-of-plane deformation may be hundreds of times larger than the paper thickness. For this large-magnitude post-buckling behavior, it is necessary to use the equations known as the *elastica*. In the equations of the *elastica*, the simplifying assumption of small deflection is not used, and the local curvature of the wrinkle is described in exact terms.

Post-buckling behavior

The model for the large-deflection buckling is shown in **Fig. 1**. The initial development of the *elastica* in the eighteenth century is credited to Euler and Lagrange. Timoshenko and Gere (*5*) provide a concise development of the post-buckling equations for application to linear, isotropic, and homogeneous materials. Although paper is neither linear, isotropic, nor homogeneous, the wrinkles described in the present study show very good agreement with the *elastica* equations.

The *elastica* allow the geometry of the wrinkle cross-section to be quantitatively described. The solid portion of the curve in Fig. 1 represents only one-fourth of a complete wrinkle. Because an entire half-wrinkle can be described by subsequently applying the *elastica*, and because the entire wrinkle is symmetrical about the wrinkle axis, the equations given by Timoshenko and Gere (*5*) are those needed to completely describe the wrinkle geometry.

The *elastica* solution is burdensome to work with because elliptic integrals form a portion of the solution. The values for the elliptic integrals are well documented (*6*). They also can be solved numerically. However, each of these processes requires considerable effort to simply describe a well-behaved function such as a wrinkle cross-section. In addition, for large wrinkles in weak materials, the *elastica* may provide a result that differs from the shape measured in the actual web material. This occurs because the *elastica* do not consider any deformation resulting from the weight of the web material. Actually, the wrinkle tends to deform slightly downward from the shape predicted by the *elastica*. This deformation could result in a slightly higher aspect ratio for the actual wrinkle.

Experimentation and results

In an effort to simplify the *elastica* equations and to characterize a wide variety of wrinkle cross-sections for repeated use in stability studies, a number of different sizes and shapes

3. General wrinkle parameters

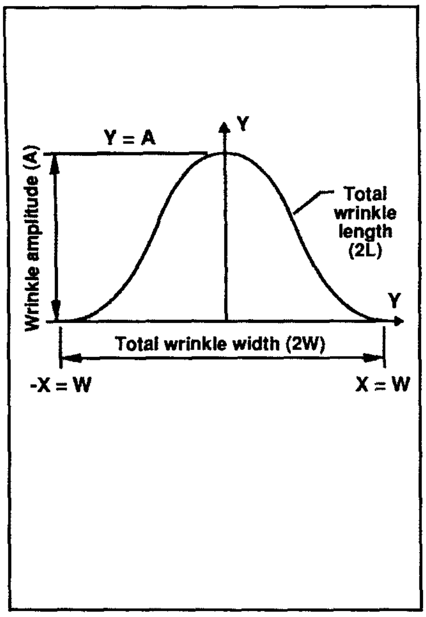

4. Measured data for three representative wrinkles

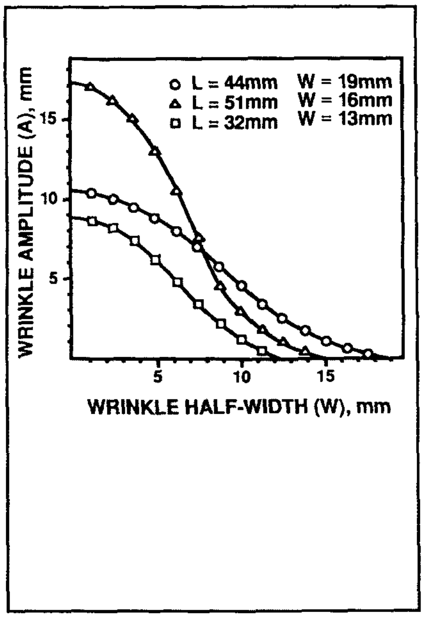

5. Normalized data for the wrinkles depicted in Fig. 4

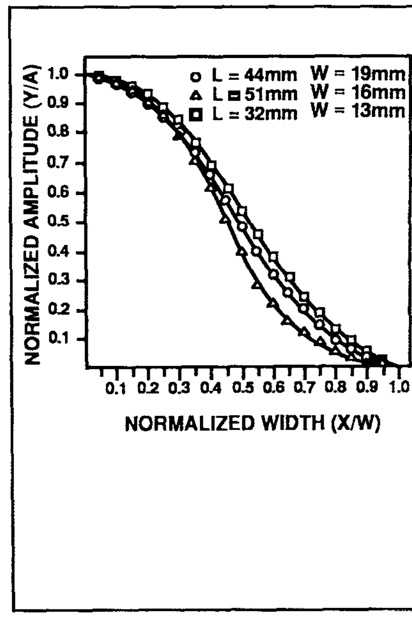

of wrinkles, in several types of paper, were created in a static situation. The samples tested were kraft paper with a caliper of 0.2 mm (8 mil) and a basis weight of 152 g/m^2, newsprint with a caliper of 0.09 mm (3.5 mil) and a basis weight of 53 g/m^2, and xerography paper with a caliper of 0.1 mm (4 mil) and a basis weight of 81 g/m^2. The apparatus for inducing the wrinkles in the kraft paper and the newsprint is shown in **Fig. 2**.

The apparatus allowed variations in the web span, web width, and shear strain. In all cases, the wrinkles were measured at the mid-span of the web. Wrinkles of different size and shape were induced by varying the span, width, and shear strain in the web. The wrinkles in the xerography paper were induced by simply subjecting the sample to shear strain by hand. The wrinkle parameters are shown in **Fig. 3**. For the purpose of this study, both wrinkle width and wrinkle length refer to measurements in the cross-machine direction. The wrinkle length is not meant to imply a measurement in the machine direction. This represents a deviation from conventional terminology.

Wrinkles of specified length and width were induced in the three types of paper. The cross-sectional shape of the wrinkle was measured for each type of paper, and the shapes were found to be the same within the accuracy of the measurement. This result was anticipated and would be expected for all web samples with sufficient stiffness to resist excessive deformation caused by the web's own weight.

Because the three types of paper exhibited the same cross-sectional geometry, newsprint was used for the remainder of the experimental studies. A series of 25 wrinkles of very different size and aspect ratio were induced in newsprint. The height of each wrinkle was measured at various points along the wrinkle width. The measurements were made by positioning a graduated straightedge under the web at the mid-span. The wrinkle width (2W) was determined to be at the points where the straightedge was tangent to the bottom of the wrinkle. These points were marked and later served to indicate the wrinkle length (2L) after the sheet was again flattened. With the wrinkle still in place, calipers were used to measure from the graduated straightedge up to the associated point on the wrinkle. Although tedious, this process required no special equipment or expertise.

Figure 4 shows data for three representative wrinkles. Because of symmetry, only one-half of the wrinkle is shown. The wrinkles were such that the maximum slope was less than vertical. This restriction is necessary to force a monotonic, single-valued function for the approximating polynomial. In the *elastica* equations, this restriction need not be enforced.

Several attempts at describing the 25 wrinkle shapes with a single polynomial failed to yield a function that accurately described the wrinkle shapes. The wrinkle parameters were then normalized with respect to the maximum magnitude of that parameter. For each measured point in the wrinkle cross-section, the x-coordinate of the point was divided by the wrinkle half-width, and the y-coordinate was divided by the maximum amplitude at the axis of symmetry. The normalized plot showed good agreement among the many wrinkles. **Figure 5** is a normalized plot of the three representative wrinkles in Fig. 4. These three normalized wrinkles represent the two extremes and the approximate average for the data scatter of all 25 measured wrinkles.

In a similar manner, the amplitude of each wrinkle at the axis of symmetry was measured as each wrinkle was developed. (With the sheet flat, the amplitude was zero.) As shear strain was induced in the web, the total wrinkle width (2W) became less than the total wrinkle length (2L), and the amplitude at the axis of symmetry was successively measured. From observations of the size of the wrinkles, it became obvious that for a total wrinkle length when flat, the amplitude of an associated wrinkle should be related to the final total wrinkle width. This was found to be true, and this relationship is shown in **Fig. 6** for the average of the 25 wrinkles. For a wrinkle with a total width (2W) which develops from a flat sheet of total length (2L), the characterized amplitude is directly related to the characterized width. The characterized parameters are different from the normalized parameters in that the characterized parameters are only dependent upon the total wrinkle length of the flat sheet and not on the maximum measured value of the parameter.

From the normalized and characterized data for the 25 wrinkles, a least-squares curve fit was performed on all the wrinkle data, resulting in two third-order polynomials. A third-order polynomial was selected because the equations of elasticity have a fourth derivative equal to zero. The input to the polynomials is the overall length of the flat sheet before wrinkling (2L) and the wrinkle width (2W). The output of the polynomials is the maximum amplitude (A) of the wrinkle at the axis of symmetry and the functional relationship (Y) between the height and width coordinates of the cross-section. The polynomials and the coefficients are given in Eqs. 1 and 2.

$$A = 2L\,\{a + b(2W/2L) + c[(2W/2L)^2] + d[(2W/2L)^3]\} \quad (1)$$

where

$a = 0.5980$

$b = -1.1112$

$c = 2.2470$

$d = -1.6933$

$$Y = A\,\{a + b(X/W) + c[(X/W)^2] + d[(X/W)^3]\} \quad (2)$$

where, for $0 < X/W < 0.5$

$a = 0.9999$

$b = -0.1725$

$c = -0.8873$

$d = -2.0992$

or, for $0.5 < X/W < 1.0$

$a = 2.1191$

$b = -5.1762$

$c = 4.2300$

$d = -1.1733$

6. Average of characterized wrinkles

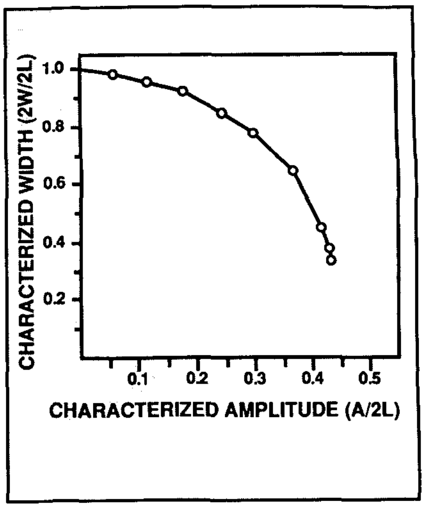

7. Comparison of analyses

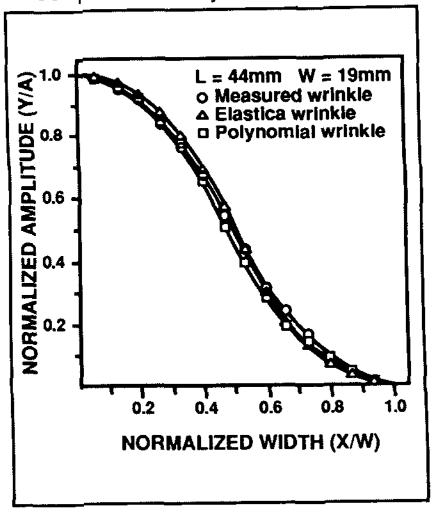

For an area of a web with known initial length prior to wrinkle formation and with known wrinkle width, the maximum amplitude (A) is first calculated from Eq. 1. Then the functional relationship describing the cross-section (Y for any X/W ratio) is calculated from Eq. 2. As can be seen from the coefficients, an exact fit between the measured wrinkle and the polynomials is not achieved. An error analysis indicates that, at any point, the curve fit deviates less than 10% from the measured values.

The polynomial relationship of the wrinkle cross-section allows a second simple analysis to be made. The polynomial relationship is a geometric function and has no material restrictions placed upon it. If the wrinkle curvature becomes large enough, the material may crease without any additional interaction from a roller. The bending stress at a point in the wrinkle cross-section is directly related to the curvature at that point. For a large deformation, the exact curvature (K) is given by Eq. 3.

$$K = |d^2y/dx^2|/[1 + (dy/dx)^2]^{3/2} \quad (3)$$

This curvature is equal to M/EI, where M is the bending moment, E is Young's modulus, and I is the moment of inertia of the bending section. In small-deformation analyses, the curvature (K) is approximated by the numerator of Eq. 3 because the slope (dy/dx) at any point is assumed to be very small, thus making the denominator equal to unity. In web wrinkling, this approximation generally is not valid. Making the simple substitution for the beam bending stress yields Eq. 4,

$$\sigma = KET/2 \quad (4)$$

where T is the web thickness. By taking the appropriate derivatives of the polynomial relationship shown in Eq. 3 and evaluating the derivatives at any point (X/W) in the cross-section, the curvature and bending stress at that point can be approximated. This stress is typically expressed for a unit dimension of the wrinkle in the machine direction.

Conclusions and applications

Figure 7 is a comparison of the theoretical wrinkle shapes as derived from the *elastica*, the experimentally measured wrinkle shapes, and the shapes predicted by the polynomial approximation. As can be seen, there is very good agreement among all three curves. From this comparison, it can be concluded that the approximating polynomial is a very easy tool for the description of wrinkle geometry. This close correlation would also indicate that in wrinkling studies, where the web material is not highly stressed, the assumption of a linear, isotropic, and homogeneous material is satisfied.

The polynomial approximation also provides a quick method for calculating the bending stress at selected points in the wrinkle cross-section. It can be seen from Fig. 6 that the characterized amplitude of a wrinkle becomes maximum at 44% of the total wrinkle length. This occurs as the slope of the wrinkle becomes vertical. This fact could prove useful in determining the geometry and limiting size of a wrinkle that has collapsed or folded onto itself during processing.

The approximating polynomial is being used in the study of the relationship between shear strain in a web and the size and shape of the resulting wrinkle. Recent work by Gehlbach *et al.* (*7*) has resulted in a method for predicting the existence of shear wrinkles based on induced shear strain. The current study can be applied to this recent work to predict the wrinkle size and shape as it relates to the shear strain present in the web span. A model can then be formulated to predict the response of the resulting wrinkle passing over a roller. This work will place an upper limit on the amount of shear strain allowable in a web span before wrinkle instability will result. Such a relationship should help determine guidelines for roller alignment and eccentricity as well as steering or guiding of the web.□

Literature cited

1. Friedrich, C. and Good, J., Tappi J. 72(2): 161(1989).
2. Wang, C., Applied Elasticity, McGraw-Hill, New York, 1953.
3. Vinson, J. R., Structural Mechanics: The Behavior of Plates and Shells, John Wiley & Sons, New York, 1974.
4. Ugural, A. C., Stresses in Plates and Shells, McGraw-Hill, New York, 1981.
5. Timoshenko, S. and Gere, J. M., Theory of Elastic Stability, McGraw-Hill, New York, 1961.
6. Standard Mathematical Tables, CRC Press, Cleveland, 1974.
7. Gehlbach, L., Kedl, D., and Good, J., Tappi J. 72(8): 129 (1989).

This material is based on work supported by the National Science Foundation under Grant No. DMC-8808298.

Received for review May 15, 1989.

Accepted Feb. 12, 1990.